AIP | Applied Physics Letters

Magnetically tunable wideband microwave filter using ferrite-based metamaterials

Ke Bi, Wenting Zhu, Ming Lei, and Ji Zhou

Citation: Applied Physics Letters **106**, 173507 (2015); doi: 10.1063/1.4918992
View online: http://dx.doi.org/10.1063/1.4918992
View Table of Contents: http://scitation.aip.org/content/aip/journal/apl/106/17?ver=pdfcov
Published by the AIP Publishing

Magnetically tunable wideband microwave filter using ferrite-based metamaterials

Ke Bi,[1] Wenting Zhu,[1] Ming Lei,[1,a)] and Ji Zhou[2]
[1]State Key Laboratory of Information Photonics and Optical Communications and School of Science, Beijing University of Posts and Telecommunications, Beijing 100876, China
[2]State Key Laboratory of New Ceramics and Fine Processing, School of Materials Science and Engineering, Tsinghua University, Beijing 100084, China

(Received 12 January 2015; accepted 12 April 2015; published online 29 April 2015)

Magnetically tunable wideband microwave filters have been designed and prepared by using ferrite-based metamaterial structures. The microwave properties of the filters have been investigated by experiments and simulations. The negative permeability appears around the ferromagnetic resonance frequency, which leads to a remarkable stopband for the bandstop filter. The bandpass filter is composed of two kinds of ferrite rods with different saturation magnetization. The bandwidth of the passband can be tuned by adjusting the saturation magnetization of the ferrite rods. Both the experimental and the simulated results show that those filters possess magnetically tunable property. This approach opens a way for designing tunable wideband microwave filters. © *2015 AIP Publishing LLC*. [http://dx.doi.org/10.1063/1.4918992]

Tunable microwave devices are essential in wideband communication and radar systems. Bandpass and bandstop filters are among the essential devices used in detecting and controlling the spectrums of radio frequency signals in communication and radar systems.[1,2] In recent years, ferromagnetic resonance (FMR)-based filters, such as yttrium iron garnet (YIG) based filters, have been studied and designed for different applications.[3–5] These ferrite filters possess the desirable capability of high-speed electronic tunability, using magnetic field, for very high carrier frequency and very large bandwidth.[6–8] Tsai *et al.*[9,10] reported a magnetically tunable wideband microwave bandstop and bandpass filters by using ferromagnetic resonance absorption in YIG/gadolinium gallium garnet-gallium arsenide (YIG/GGG-GaAs) layer structures. However, the bandpass filter was prepared by using a pair of bandstop filters in cascade, which increases the complexity of the structure.

Metamaterials are a class of artificial materials with subwavelength functional electromagnetic microstructures.[11] Through regulating the interaction between the electromagnetic wave and the artificial structures, metamaterials provide a physical platform to controlling electromagnetic waves.[12] Recently, ferrite-based metamaterials with magnetically tunable properties have been widely discussed in theory, and various structures have been proposed.[13–15] By interacting with electromagnetic wave, ferrite based metamaterials provide negative permeability when the FMR takes place.[16–18] Proper control of the lattice arrangement, unit cell geometry, and material parameters allows control over the effective permittivity and permeability of the metamaterials.[19] When the negative permeability appears, the stopband will be obtained. In previous work, our group experimentally and numerically studied the electromagnetic properties of the metamaterials consisting of metallic wires and ferrite rods with various $4\pi M_s$, and obtained negative effective permeability in magnetic resonance mode.[20] In this work, we demonstrate a magnetically tunable wideband microwave filter using ferrite-based metamaterials. The microwave transmission properties of the ferrite-based metamaterials can be influenced by the saturation magnetization $4\pi M_s$ of the ferrite rods. Hence, the frequency range of the stopband is not only tuned by the applied magnetic field but also adjusted by the $4\pi M_s$ of the ferrite rods. A wideband microwave bandpass filter composed of ferrite rods with different $4\pi M_s$ has also been prepared. The bandwidth of the passband can be tuned by the $4\pi M_s$ of the ferrite, which opens a way to design filter with more freedom.

The commercial YIG rods were sliced with dimensions of $1 \times 1 \times 10\,\text{mm}^3$. The linewidth ΔH and relative permittivity ε_r of the YIG rods are 35 Oe and 14.5. The saturation magnetizations $4\pi M_s$ are 1200 Gs, 1400 Gs, 1600 Gs, and 1950 Gs, respectively. The magnetically tunable microwave bandstop filter was fabricated by inserting the ferrite rods with the same $4\pi M_s$ into a Teflon substrate, as shown in Figure 1(a). The magnetically tunable microwave bandpass filter was fabricated by inserting the ferrite rods with the different $4\pi M_s$ into a Teflon substrate, as shown in Figure 1(b). The distance d between the two ferrite rods with different $4\pi M_s$ is 0.6 mm. The size of the unit cell for all the filters is $4 \times 4 \times 10\,\text{mm}^3$. By interacting with the magnetic field of an incoming electromagnetic wave, FMR can arise in ferrite rods under an applied magnetic field. The FMR frequency can be expressed by

$$\omega_r = \gamma\sqrt{[H_0 + (N_x - N_z)4\pi M_s][H_0 + (N_y - N_z)4\pi M_s]}, \quad (1)$$

where γ is the gyromagnetic ratio; $4\pi M_s$ is the saturation magnetization; H_0 is the applied magnetic field; N_x, N_y, and N_z are the demagnetization factors for x, y, and z directions, respectively. From Eq. (1), one observes that the FMR frequency increases as the H_0 or $4\pi M_s$ increases. Based on this

a)Author to whom correspondence should be addressed. Electronic address: mlei@bupt.edu.cn.

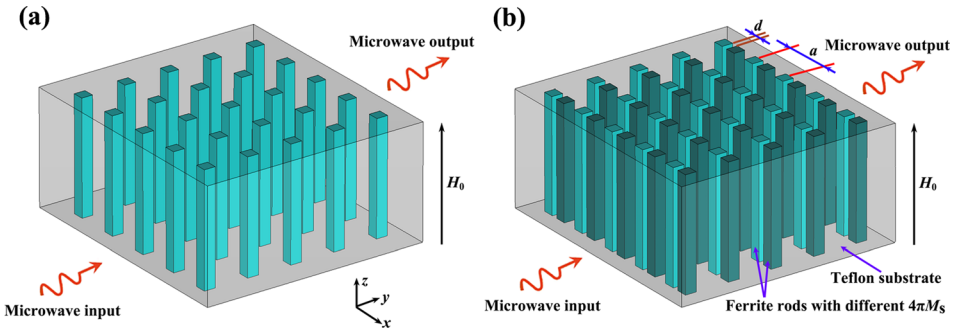

FIG. 1. Schematic diagrams of the magnetically tunable microwave (a) bandstop filter and (b) bandpass filter using ferrite-based metamaterial structure.

theory, the filter with magnetically tunable and broad bandwidth can be designed.

In order to understand the electromagnetic properties of the magnetically tunable microwave filter, we simulated the transmission spectra of the one ferrite rod unit cell by using the commercial time-domain package CST Microwave Studio TM. The schematic diagram of one ferrite rod unit cell is shown in Figure 2(a). All the parameters of the ferrite rod are the same as those in the experiments. A plane wave is assumed for the incident electromagnetic field with polarization conditions, which corresponds to the electric field direction along the z axis and to the magnetic field direction along the x axis, respectively. The effective permeability of the unit cell for the filter was extracted from the simulated scattering parameters using a well-developed retrieval algorithm.[21–23] For the unit cell with a series of applied magnetic filed H_0, the dependence of the calculated effective permeability on frequency is shown in Figure 2(b). First, because the FMR take places, the unit cell exhibits a Lorentz type dispersion and the negative effective permeability appears around the FMR frequency. Second, as H_0 increases from 2000 Oe to 2600 Oe, the frequency related to negative permeability increases. For the unit cell with a series of saturation magnetization $4\pi M_s$, the dependence of the calculated effective permeability on frequency is shown in Figure 2(c). It can be seen that the frequency related to negative permeability increases as the $4\pi M_s$ increases from 1200 Oe to 1950 Oe. The behavior in simulated results is consistent with that predicted by Eq. (1).

The filters were characterized by the microwave measurement system composed of a vector network analyzer (HP 8720ES), an X-band rectangular waveguide (WR90, $22.86 \times 10.16\,\text{mm}^2$), and an electromagnet. The details of the microwave measurement system were described in elsewhere.[20] As shown in Figure 1, the propagation of the incident electromagnetic wave was along the y axis, and the electric field and magnetic field were along the z and x axes, respectively. The bias magnetic field provided by the electromagnets was applied in the z direction, which can be adjusted by input current. Figure 3(a) shows the measured transmission spectra for the magnetically tunable microwave bandstop filter with a series of H_0. The $4\pi M_s$ of the ferrite rods is 1950 Oe. It can be seen that the stopband center frequency ranges from 8.75 GHz to10.37 GHz for H_0 in the range of 2000–2600 Oe, tuning at the rate of 2.7 GHz/kOe. As an example, when $H_0 = 2200$ Oe, the experimental data exhibits a -3 dB stop bandwidth as large as 500 MHz, a peak absorption of -47 dB, and an out-of-stopband insertion loss of -1 dB. Figure 3(b) shows the measured transmission spectra for the magnetically tunable microwave bandstop

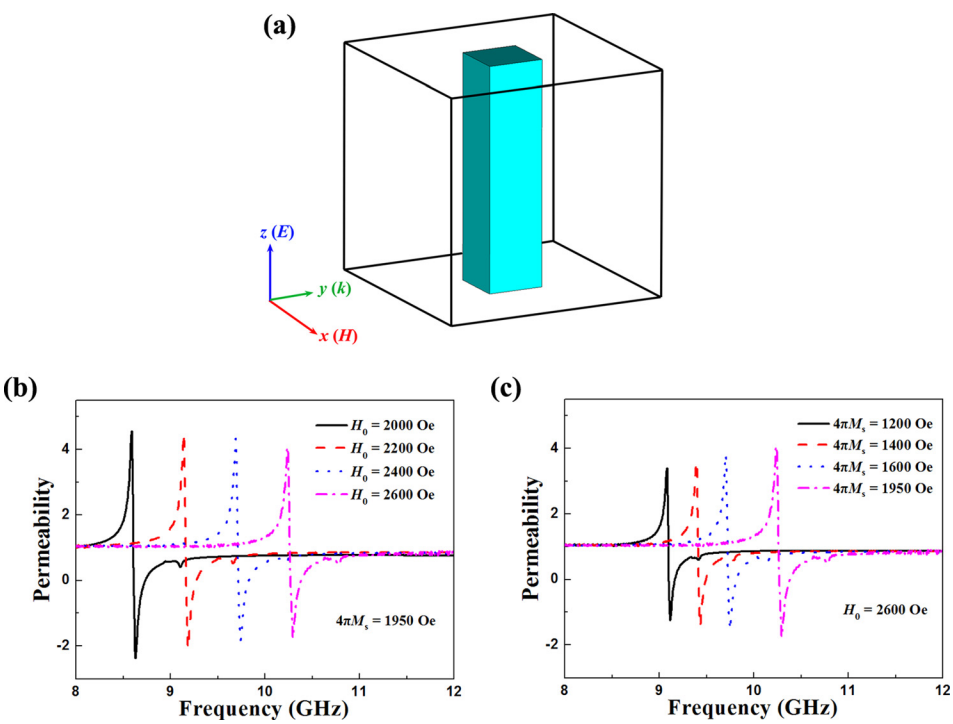

FIG. 2. (a) Schematic diagram of one ferrite rod unit cell for the bandstop filter; real part of the effective permeability retrieved from the simulated scattering parameters for the unit cell with a series of (b) H_0 and (c) $4\pi M_s$.

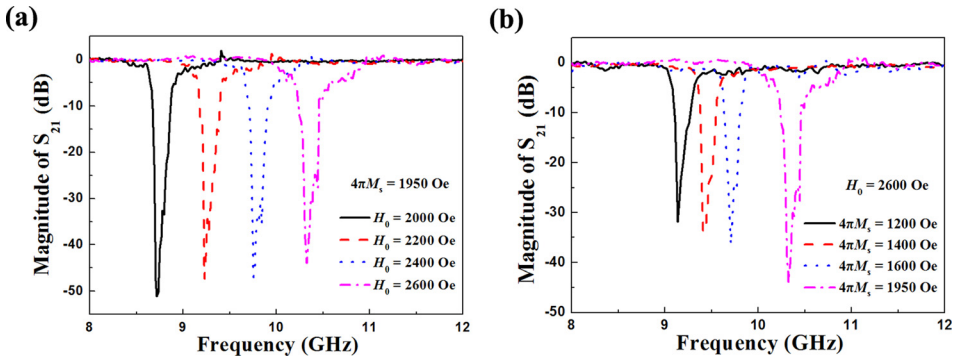

FIG. 3. Measured transmission spectra for the magnetically tunable microwave bandstop filter with a series of (a) H_0 and (b) $4\pi M_s$.

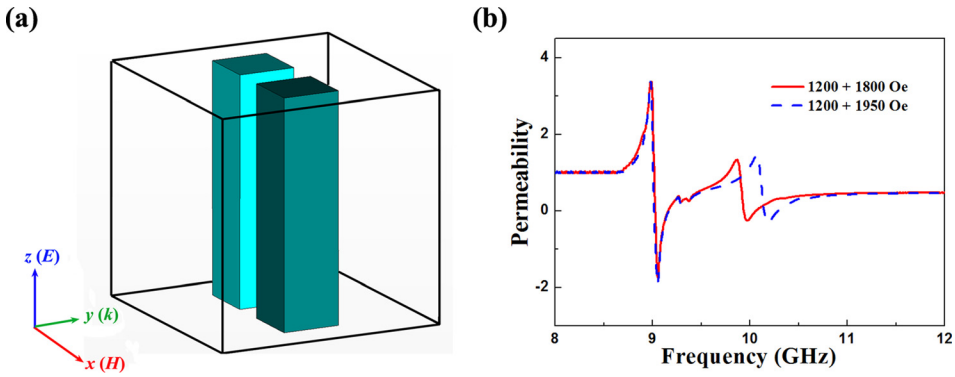

FIG. 4. (a) Schematic diagram of two ferrite rods unit cell for the bandpass filter; (b) real part of the effective permeability retrieved from the simulated scattering parameters for the ferrite rods with different $4\pi M_s$.

filter at $H_0 = 2600$ Oe with a series of $4\pi M_s$. The stopband center frequency increases as the $4\pi M_s$ increases. Based on the above experimental data and the simulated results in Figure 2, we can see that the stopband frequency region is where the permeability shows negative values. The bandstop filter shows a magnetically tunable behavior.

Figure 4(a) shows the schematic diagram of two ferrite rods unit cell for the bandpass filter. The two ferrite rods have same size. The $4\pi M_s$ of one ferrite rod is set at 1200 Oe, and that of the other ferrite rod is 1800 and 1950 Oe, respectively. The dependence of the effective permeability retrieved from the simulated scattering parameters on frequency is shown in Figure 4(b). For all cases, two Lorentz type dispersions appear at 8–12 GHz, which indicates two FMRs take place. Around two FMR frequencies, two negative permeability frequency regions appear. Based on the FMR theory and the simulated data shown in Figure 4(b), we can conclude that the dispersion controlled by the rod $4\pi M_s = 1200$ Oe has not changed, and the dispersion controlled by the other rod moves to higher frequency region as its $4\pi M_s$ increases from 1800 to 1950 Oe. Hence, by adjusting the $4\pi M_s$ of ferrite rods, we can get a material with two negative permeability frequency regions at any frequency, which demonstrates the bandpass filter with tunable bandwidth can be obtained.

Figure 5(a) shows the measured transmission spectra for the magnetically tunable microwave bandpass filter at 2600 Oe. When the $4\pi M_s$ of ferrite rods are 1200 Oe and 1800 Oe, the measured transmission characteristics at the center frequency of 9.6 GHz shows a −3 dB bandwidth as large as 700 MHz, an out-of-band rejection of −30 dB, and an insertion loss of −2.2 dB. When the $4\pi M_s$ of ferrite rods are 1200 Oe and 1950 Oe, the bandwidth of the passband increases to 850 MHz. The experimental results are consistent with that in simulated ones. We can see that the bandwidth of the passband can be tuned by the $4\pi M_s$ of ferrite rods. Figure 5(b) shows the measured transmission spectra for the magnetically tunable microwave bandpass filter with a series of H_0. The $4\pi M_s$ of ferrite rods are 1200 Oe and 1950 Oe. The passband center frequency increases as the H_0 increases, which shows a magnetically tunable property.

In conclusion, the magnetically tunable wideband microwave bandstop and bandpass filters have been prepared by using ferrite-based metamaterials. Both the bandstop and

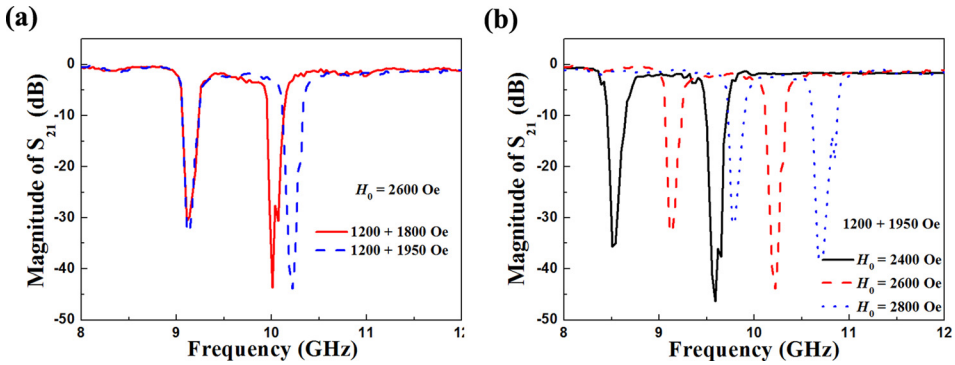

FIG. 5. Measured transmission spectra for the magnetically tunable microwave bandpass filter with (a) different $4\pi M_s$ and (b) a series of H_0.

bandpass filters show the magnetically tunable property, large bandwidth, and low insertion loss. In addition, the bandpass filter demonstrates a bandwidth tunable property. The experimental results are in good agreement with the simulation ones. This work provides a way to fabricate the microwave bandstop and bandpass filters, which has greater potential for frequency-hopping wideband microwave communication and signal processing systems.

This work was supported by the National Natural Science Foundation of China under Grant Nos. 51402163, 61376018, 51032003, 11274198, 51102148, and 51221291; the China Postdoctoral Science Foundation under Grant Nos. 2013M530042 and 2014T70075; and the Fundamental Research Funds for the Central Universities under Grant No. 2015RC18.

[1]G. L. Matthaei, IEEE Trans. Microw. Theory Tech. **13**, 203 (1965).
[2]I. C. Hunter, L. Billonet, B. Jarry, and P. Guillon, IEEE Trans. Microw. Theory Tech. **50**, 794 (2002).
[3]B. K. Kuanr, I. R. Harward, R. T. Deiotte, R. E. Camley, and Z. Celinski, J. Appl. Phys. **97**, 10Q103 (2005).
[4]Y. Guo, F. R. Shen, and X. Y. Chen, Appl. Phys. Lett. **101**, 012410 (2012).
[5]H. Zhang, P. Guo, S. J. Chang, and J. H. Yuan, Chin. Phys. Lett. **25**, 3898 (2008).
[6]X. Yang, Y. Gao, J. Wu, S. Beguhn, T. X. Nan, Z. Y. Zhou, M. Liu, and N. X. Sun, IEEE Trans. Magn. **49**, 5485 (2013).
[7]X. Yang, J. Wu, S. Beguhn, T. Nan, Y. Gao, Z. Zhou, and N. X. Sun, IEEE Microwave Wireless Compon. Lett. **23**, 184 (2013).
[8]I. Harward, R. E. Camley, and Z. Celinski, Appl. Phys. Lett. **105**, 173503 (2014).
[9]C. S. Tsai, G. Qiu, H. Gao, L. W. Yang, G. P. Li, S. A. Nikitov, and Y. Gulyaev, IEEE Trans. Magn. **41**, 3568 (2005).
[10]G. Qiu, C. S. Tsai, B. S. T. Wang, and Y. Zhu, IEEE Trans. Magn. **44**, 3123 (2008).
[11]R. A. Shelby, Science **292**, 77 (2001).
[12]T. Paul, C. Menzel, C. Rockstuhl, and F. Lederer, Adv. Mater. **22**, 2354 (2010).
[13]Y. He, P. He, V. G. Harris, and C. Vittoria, IEEE Trans. Magn. **42**, 2852 (2006).
[14]G. Dewar, New J. Phys. **7**, 161 (2005).
[15]H. Zhao, J. Zhou, L. Kang, and Q. Zhao, Opt. Express **17**, 13373 (2009).
[16]P. He, J. Gao, Y. Chen, P. V. Parimi, C. Vittoria, and V. G. Harris, J. Phys. D: Appl. Phys. **42**, 155005 (2009).
[17]F. Xu, Y. Bai, F. Ai, L. Qiao, H. Zhao, and J. Zhou, J. Phys. D: Appl. Phys. **42**, 065416 (2009).
[18]J. N. Gollub, J. Y. Chin, T. J. Cui, and D. R. Smith, Opt. Express **17**, 2122 (2009).
[19]K. Bi, J. Zhou, H. Zhao, X. Liu, and C. Lan, Opt. Express **21**, 10746 (2013).
[20]K. Bi, J. Zhou, X. Liu, C. Lan, and H. Zhao, Prog. Electromagn. Res. **140**, 457 (2013).
[21]D. R. Smith, S. Schultz, P. Markoš, and C. M. Soukoulis, Phys. Rev. B **65**, 195104 (2002).
[22]C. Croënne, B. Fabre, D. Gaillot, O. Vanbésien, and D. Lippens, Phys. Rev. B **77**, 125333 (2008).
[23]X. Chen, T. M. Grzegorczyk, B. Wu, J. Pacheco, and J. A. Kong, Phys. Rev. E **70**, 016608 (2004).